



## Air-stable -conjugated amorphous copolymer field-effect transistors with high mobility of 0.3 cm<sup>2</sup>/Vs

Georgakopoulos, S.; Gu, Y.; Nielsen, Martin Meedom; Shkunov, M.

*Published in:*  
Applied Physics Letters

*Link to article, DOI:*  
[10.1063/1.4767921](https://doi.org/10.1063/1.4767921)

*Publication date:*  
2012

*Document Version*  
Publisher's PDF, also known as Version of record

[Link back to DTU Orbit](#)

*Citation (APA):*  
Georgakopoulos, S., Gu, Y., Nielsen, M. M., & Shkunov, M. (2012). Air-stable -conjugated amorphous copolymer field-effect transistors with high mobility of 0.3 cm<sup>2</sup>/Vs. *Applied Physics Letters*, 101(21), 213305. <https://doi.org/10.1063/1.4767921>

---

### General rights

Copyright and moral rights for the publications made accessible in the public portal are retained by the authors and/or other copyright owners and it is a condition of accessing publications that users recognise and abide by the legal requirements associated with these rights.

- Users may download and print one copy of any publication from the public portal for the purpose of private study or research.
- You may not further distribute the material or use it for any profit-making activity or commercial gain
- You may freely distribute the URL identifying the publication in the public portal

If you believe that this document breaches copyright please contact us providing details, and we will remove access to the work immediately and investigate your claim.

## Air-stable $\pi$ -conjugated amorphous copolymer field-effect transistors with high mobility of 0.3 cm<sup>2</sup>/Vs

S. Georgakopoulos, Y. Gu, M. M. Nielsen, and M. Shkunov

Citation: *Appl. Phys. Lett.* **101**, 213305 (2012); doi: 10.1063/1.4767921

View online: <http://dx.doi.org/10.1063/1.4767921>

View Table of Contents: <http://apl.aip.org/resource/1/APPLAB/v101/i21>

Published by the [American Institute of Physics](#).

---

### Related Articles

Investigation of an anomalous hump in gate current after negative-bias temperature-instability in HfO<sub>2</sub>/metal gate p-channel metal-oxide-semiconductor field-effect transistors

*Appl. Phys. Lett.* **102**, 012103 (2013)

Study of individual phonon scattering mechanisms and the validity of Matthiessen's rule in a gate-all-around silicon nanowire transistor

*J. Appl. Phys.* **113**, 014501 (2013)

High performance CMOS-like inverter based on an ambipolar organic semiconductor and low cost metals

*AIP Advances* **3**, 012101 (2013)

Dynamics of a polariton condensate transistor switch

*Appl. Phys. Lett.* **101**, 261116 (2012)

High responsivity of amorphous indium gallium zinc oxide phototransistor with Ta<sub>2</sub>O<sub>5</sub> gate dielectric

*Appl. Phys. Lett.* **101**, 261112 (2012)

---

### Additional information on *Appl. Phys. Lett.*

Journal Homepage: <http://apl.aip.org/>

Journal Information: [http://apl.aip.org/about/about\\_the\\_journal](http://apl.aip.org/about/about_the_journal)

Top downloads: [http://apl.aip.org/features/most\\_downloaded](http://apl.aip.org/features/most_downloaded)

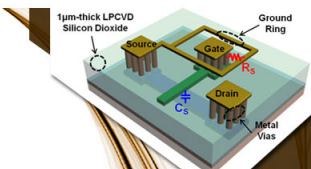
Information for Authors: <http://apl.aip.org/authors>

## ADVERTISEMENT

**AIP** | Applied Physics  
Letters


**EXPLORE WHAT'S  
NEW IN APL**

**SUBMIT YOUR PAPER NOW!**



**SURFACES AND  
INTERFACES**

Focusing on physical, chemical, biological, structural, optical, magnetic and electrical properties of surfaces and interfaces, and more...



**ENERGY CONVERSION  
AND STORAGE**

Focusing on all aspects of static and dynamic energy conversion, energy storage, photovoltaics, solar fuels, batteries, capacitors, thermoelectrics, and more...

# Air-stable $\pi$ -conjugated amorphous copolymer field-effect transistors with high mobility of $0.3 \text{ cm}^2/\text{Vs}$

S. Georgakopoulos,<sup>1</sup> Y. Gu,<sup>2</sup> M. M. Nielsen,<sup>3</sup> and M. Shkunov<sup>1</sup>

<sup>1</sup>Advanced Technology Institute, Electronic Engineering, University of Surrey, Guildford GU2 7XH, United Kingdom

<sup>2</sup>Niels Bohr Institute and Nanoscience Center, Universitetsparken 5, 2100 Kobenhavn, Denmark

<sup>3</sup>Riso DTU, Materials Research Division, Frederiksborgvej 399, P.O. Box 49, DK-4000 Roskilde, Denmark

(Received 29 July 2012; accepted 2 November 2012; published online 20 November 2012; corrected 18 December 2012)

We have fabricated organic bottom-contact top-gate field-effect transistors with an indenofluorene-phenanthrene co-polymer semiconductor, exhibiting ON/OFF ratio of  $10^7$  and uncommonly high mobility for an amorphous conjugated polymer of up to  $0.3 \text{ cm}^2/\text{Vs}$ . Lack of crystallinity in this material is indicated by atomic force microscopy, grazing incidence wide angle X-ray scattering, and differential scanning calorimetry data. Nevertheless, fitting transistor data to the Gaussian disorder model gives low energetic disorder of  $\sigma = 48 \text{ meV}$  and high prefactor mobility  $\mu_0 = 0.67 \text{ cm}^2/\text{Vs}$ . The measured transistor mobility is also exceptionally stable in ambient conditions, decreasing only by approximately 15% over two months. © 2012 American Institute of Physics. [<http://dx.doi.org/10.1063/1.4767921>]

The ease of processing of polymers from solution is an attractive feature for the fabrication of electronic devices utilizing low-cost, large-area, high-throughput printing techniques. The electrical performance of  $\pi$ -conjugated polymer semiconductors, however, and specifically the charge carrier mobility, is relatively low. Commonly used high-performance polycrystalline solution-processable organic semiconductors, such as 6,13-bis(triisopropylsilyl)ethynylpentacene (TIPS-pentacene) and poly[2,5-bis(3-alkylthiophen-2-yl)thieno(3,2-b)thiophene] (PBTTT), exhibit field-effect saturation mobilities of up to  $1 \text{ cm}^2/\text{Vs}$  and  $0.6 \text{ cm}^2/\text{Vs}$ , respectively.<sup>1,2</sup> As the benchmark for practical devices is considered to be  $0.1 \text{ cm}^2/\text{Vs}$ ,<sup>3</sup> the mobility of organic semiconductors is currently sufficient for commercial exploitation.

However, crystalline organic semiconductors rely on extensive  $\pi$ -stacking for efficient charge transport, and thus the mobility is proportional to the degree of crystallinity in the semiconductor film.<sup>4,5</sup> Crystallinity in solution deposited thin films can be challenging to reproduce, resulting in a wide spread of mobilities across similarly processed devices.<sup>6,7</sup> On the contrary, amorphous polymers lack long range order, resulting in lower but highly reproducible mobilities. Good examples of the latter case include polytriarylamine and polytriphenylamine homopolymers and copolymers with mobilities in the range of  $3 \times 10^{-3}$  to  $0.03 \text{ cm}^2/\text{Vs}$ .<sup>8–11</sup>

Additionally, organic semiconductors are sensitive to ambient conditions, specifically humidity and oxygen.<sup>12,13</sup> Effects of humidity on transistors are significantly reduced by utilizing highly hydrophobic dielectric insulators.<sup>14,15</sup> Effects of oxidation are limited in semiconductor materials of higher ionization potential (IP),<sup>16,17</sup> which tend to be air-stable with IPs in excess of approximately 5.3 eV.<sup>18,19</sup>

Amorphous high IP  $\pi$ -conjugated polymers represent an attractive class of semiconductor materials for printed p-type transistors. In the present work, we demonstrate field-effect transistors (FET) utilizing an amorphous  $\pi$ -conjugated

indenofluorene-phenanthrene copolymer (PIFPA) (structure in Fig. 1, synthesis described elsewhere<sup>20</sup>) with field-effect saturation mobility of up to  $0.3 \text{ cm}^2/\text{Vs}$  and high IP of  $5.79 \pm 0.1 \text{ eV}$ . The IP was obtained by cyclic voltammetry on a Princeton Applied Research VersaSTAT 4.

FETs were fabricated in bottom-contact, top-gate configuration (Fig. 1) with channel length  $L = 10 \mu\text{m}$  and width  $W = 1 \text{ cm}$ . Gold source and drain electrodes were patterned on Corning 1737 glass substrates by DC magnetron

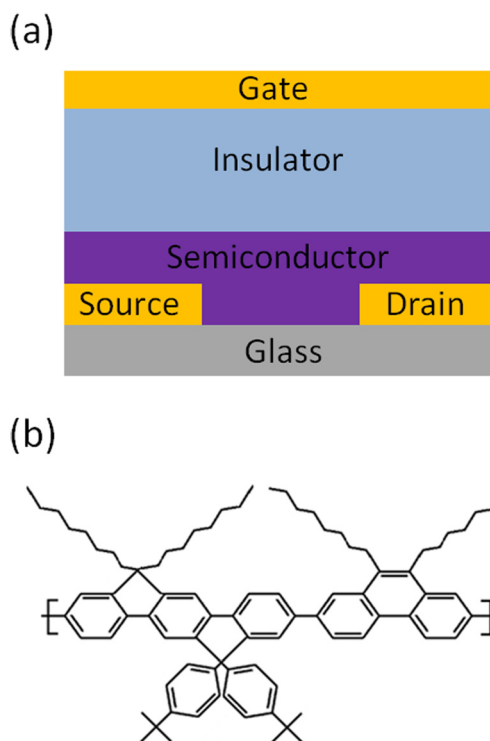


FIG. 1. (a) Structure of field-effect transistor used. (b) Chemical structure of indenofluorene-triarylamine copolymer (PIFPA).

sputtering, photolithography, and I:KI:H<sub>2</sub>O etching, followed by rinsing with acetone and isopropanol and light oxygen plasma ashing. Source/drain contacts were established with the high IP semiconductor by treating Au electrodes with a thiol self-assembled monolayer (SAM). Samples were immersed in pentafluorobenzenethiol (PFBT) in ethanol (1 mM, 15 min), followed by rinsing with ethanol and drying with pressurized nitrogen, resulting in an effective workfunction increase of up to 0.9 eV as compared to bare Au surface. Measurements were taken with a McAllister Kelvin Probe KP6500 in air. The workfunction difference between PFBT-treated Au and sputtered Cr thin film was measured, and the workfunction of the Cr sample was assumed to be 4.5 eV<sup>21</sup> to calculate the absolute value for Au-PFBT. PIFPA was spin-coated from anhydrous toluene solution (7.5 mg/ml) and annealed at 100 °C for 5 min. Highly hydrophobic Cyt<sup>TM</sup> was spin-coated and annealed (100 °C, 10 min) to form the insulating layer of thickness 1 μm and calculated capacitance

per unit area 1.85 nF cm<sup>-2</sup>. Au gate electrodes were deposited by thermal evaporation through a shadow mask (thickness 40 nm). FETs were fabricated, stored, and characterized in ambient conditions. Electrical characterization was performed with a Keithley 4200-SCS. Field-effect mobilities were extracted with the standard MOSFET model as described in previous work.<sup>18</sup>

Atomic force microscopy (AFM) images (Figs. 2(a) and 2(b)) from annealed PIFPA thin films display limited coalescence with lack of any consistent grain structures that are commonly observed in crystalline polymers. Images were taken on a Veeco Dimension 3000 with PPP-NCH tips (8 nm radius) in tapping mode. Additionally, differential scanning calorimetry (DSC) measurements (Fig. 2(e)) show no detectable heat flow peaks, indicating the lack of physical phase transitions.

Thin film copolymer samples (100 nm thick) on Si/SiO<sub>2</sub> substrates for XRD measurements were prepared in the same

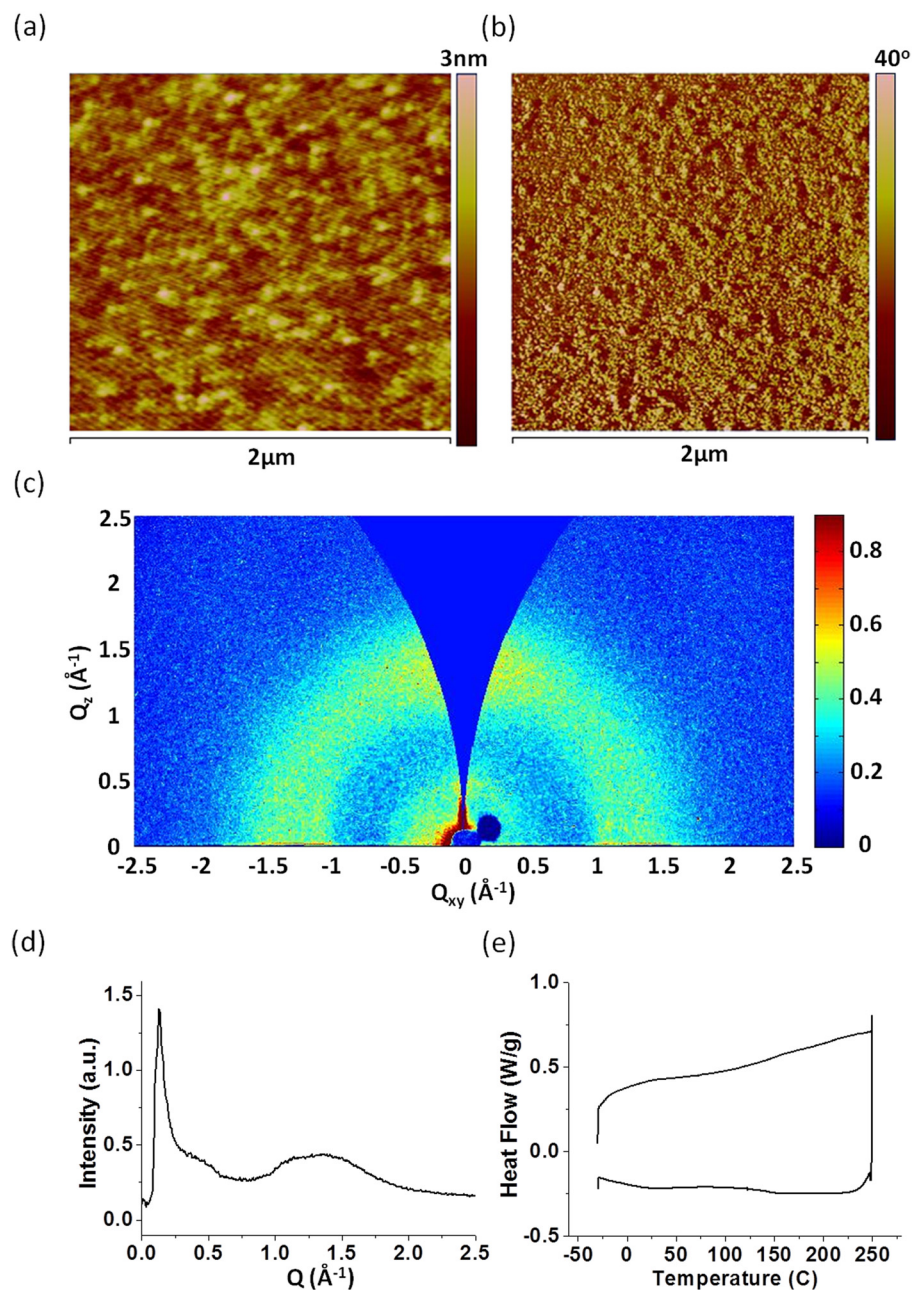


FIG. 2. Tapping mode AFM (a) height and (b) phase image of annealed PIFPA surface. (c) GIWAXS signal remapped into cylindrical reciprocal space coordinates. (d) XRD signal intensity vs scattering vector and (e) DSC characteristic of PIFPA.



way as FET samples to ensure the consistency of results. The films were examined by grazing incidence wide-angle X-ray scattering (GIWAXS) at the X-ray facility at the Technical University of Denmark, Risø. Scattering from the sample substrate was suppressed by setting the sample surface at an angle of  $0.18^\circ$  to the X-ray beam, smaller than the critical angle (approx  $0.22^\circ$  for Si/SiO<sub>2</sub>) for total external reflection from the sample substrate. The scattered intensity was recorded on 2D X-ray photon-sensitive image plates. The results were obtained with CuK $\alpha$  radiation corresponding to  $1.54 \text{ \AA}$  wavelength with  $\sim 14 \text{ h}$  exposure time to enable the detection of even very weak signals. This should be compared to typical exposure times of less than an hour in the case of crystalline samples. The signal was mapped into reciprocal space coordinates relative to the sample substrate orientation, and signal intensity was integrated azimuthally to give signal intensity versus scattering vector plots (Figs. 2(c) and 2(d), respectively). The data generally showed no evidence of sample crystallinity, and only amorphous diffuse rings were observed. The two broad distributions centred at  $0.4 \text{ \AA}^{-1}$  and  $1.3 \text{ \AA}^{-1}$ , corresponding to distances of  $15.7 \text{ \AA}$  and  $4.83 \text{ \AA}$ , respectively, are too broad and weak to be ascribed to a particular distribution of characteristic distances in the copolymer film. The sharp intensity feature below  $0.2 \text{ \AA}^{-1}$  originates from the reflection of the direct beam by the substrate surface, and does not describe a texturing of the copolymer material. The most prominent diffraction feature is a broad diffuse ring, showing a slight intensity increase towards vertical scattering direction with respect to the substrate surface (Fig. 2(c)). This feature is visible as a broad “hump” between  $1$  and  $1.6 \text{ \AA}^{-1}$  (Fig. 2(d)), possibly having some contribution from molecular textures with possible intermolecular distances of  $4.2\text{--}4.6 \text{ \AA}$ , which might include  $\pi$ - $\pi$  stacking distances. While the set up does not allow us to rule out the existence of very small ( $< 5 \text{ nm}$ ) crystalline domains, the lack of any distinct diffraction peaks, strongly suggests that the copolymer samples can be considered as amorphous.

The PIFPA FETs exhibit high quality transfer characteristics (Fig. 3(a)) with ON/OFF ratios in excess of  $10^7$ , near-zero turn-on voltage, subthreshold swing of  $0.25\text{--}1.5 \text{ V/decade}$ , and no hysteresis for forward and reverse gate voltage sweeps. The initial mobility in the saturation regime is  $0.3 \text{ cm}^2/\text{Vs}$  and in the linear regime  $0.13 \text{ cm}^2/\text{Vs}$ . The mobility in the linear regime is underestimated due to high source/drain-semiconductor contact resistance. In addition, slight non-linearity of the output characteristic at near-zero drain voltage is noticeable in Fig. 3(b). This dependence is indicative of small non-linear component of contact resistance that could also lead to underestimation of linear regime mobility.

The mobility monitored for one transistor over a period of two months was found to be generally stable, with degradation of approximately 15% over the first three weeks ( $0.3$  to  $0.25 \text{ cm}^2/\text{Vs}$ ) and no detectable degradation over the last five weeks of the characterization period (Fig. 3(c)). In other work with low- $k$  insulator PIFPA FETs, the measured mobility in air was  $0.2 \text{ cm}^2/\text{Vs}$ .<sup>22</sup>

Charge transport in disordered conjugated polymers is typically described by the Gaussian disorder model (GDM) proposed by Bassler.<sup>23</sup> The GDM is a semi-empirical Monte-Carlo (MC) simulation based model that describes thermally

activated charge hopping between localized sites, assuming a Gaussian energetic distribution characterized by the energetic disorder parameter  $\sigma$ , prefactor mobility in the absence of energetic disorder (infinite temperature)  $\mu_0$ , spatial disorder characterized by the dimensionless parameter  $\Sigma$ , and constant  $C$ , which is related to the hopping distance between sites. The GDM is described by Eq. (1), where  $k$  is Boltzmann's constant,  $T$  is the absolute temperature, and  $F$  is the magnitude of the electric field

$$\mu = \mu_0 \exp \left[ - \left( \frac{2\sigma}{3kT} \right)^2 \right] \exp \left[ C\sqrt{F} \left( \left( \frac{\sigma}{kT} \right)^2 - \Sigma \right) \right]. \quad (1)$$

To gain insight on the correlation of Gaussian energetic disorder and charge transport in PIFPA, FET variable temperature measurements were undertaken in vacuum in dark, for a temperature range of  $130$  to  $340 \text{ K}$  in steps of  $30 \text{ K}$ . The sample was measured from low to high temperatures and given  $10$  to  $15 \text{ min}$  to reach thermal equilibrium for each data point counting from the time when the temperature sensor showed a reading of  $\pm 1 \text{ K}$  from the desired temperature. The field-effect peak saturation mobility was extracted at each temperature and the natural logarithm of the mobility  $\ln(\mu_{\text{SAT}})$  was plotted against inverse square temperature ( $1000/T^2$ ) (Fig. 3(d)).

In the electric field range of  $2.5 \times 10^3$  to  $4 \times 10^4 \text{ V/cm}$ , the measured field dependence was weak, which is consistent with previous reports on temperature and field dependence of time of flight (TOF) mobility for PIFPA at even higher fields of  $1 \times 10^5$  to  $2 \times 10^5 \text{ V/cm}$ .<sup>24</sup> Consequently, to simplify analysis, field dependence described by the last term of Eq. (1) was ignored. A linear fit of  $\ln(\mu_{\text{SAT}})$  versus  $1/T^2$  was applied to the data points over higher temperatures. The energetic disorder parameter  $\sigma$  was extracted from the slope, and prefactor mobility was obtained from the y-axis intercept at infinitely high temperature ( $1/T^2 \rightarrow 0$ ) in Fig. 3(d). The extracted values were  $\sigma = 48 \pm 3 \text{ meV}$  and  $\mu_0 = 0.67 \pm 0.01 \text{ cm}^2 \text{ V}^{-1} \text{ s}^{-1}$ . The

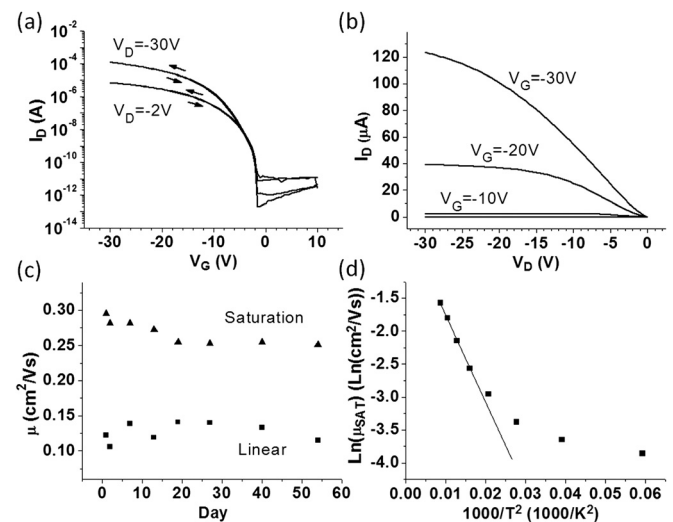


FIG. 3. Field effect transistor (a) forward and reverse transfer characteristic, (b) output characteristic, (c) peak saturation and linear mobility progression over time, measured in ambient conditions, (d)  $\ln \mu$  vs  $1000/T^2$  dependence. Simplified GDM model is applied to the linear part of the plot to extract  $\sigma$  and  $\mu_0$ .

data points over lower temperatures (190 K and below) deviate from the  $1/T^2$  fit of the GDM model and the mobility at low temperatures becomes weakly dependent on temperature.

Similar behaviour has been observed for numerous organic semiconductors including poly(9,9'-dioctylfluorene) (PFO), poly(3-hexylthiophene) (P3HT), TIPS-pentacene, PBTTT, and pentacene.<sup>25–28</sup> For PFO, the deviation from a straight line at low temperatures was explained as a transition of charge transport from non-dispersive to dispersive. For P3HT, TIPS-pentacene, and PBTTT, similar deviation was explained as a transition from thermally activated hopping to temperature independent hopping dominated by tunnelling, and the data were found to be in agreement with the Luttinger Liquid model of one-dimensional metals, which predicts weak temperature dependence at low temperatures and high electric fields.

The above value for  $\sigma$  is higher than the  $\sigma = 42$  meV reported for PIFPA TOF measurements,<sup>17</sup> as expected due to the energetic disorder broadening caused by the low- $k$  insulator-semiconductor interface in FETs.<sup>29</sup> These  $\sigma$  values are remarkably low as compared to other organic semiconductors, with  $\sigma$  values in the range of 50–150 meV.<sup>30</sup> Most examples for conjugated polymers have  $\sigma$  of 57 meV or higher and prefactor mobilities in the range of  $10^{-3}$  to  $0.1$  cm<sup>2</sup>/Vs based on TOF data for polyfluorenes, polytriarylamines, poly[2-methoxy-5-(2'-ethylhexyloxy)-p-phenylene vinylene] (MEH-PPV), and P3HT.<sup>25,28,31–33</sup> The low value of  $\sigma$  in PIFPA indicates a narrow energetic distribution of hopping sites within the density of states, and this is directly related to a more efficient hopping mechanism leading to higher charge carrier mobility. Moreover, the prefactor mobility  $\mu_0$  is associated with wavefunction overlap between neighbouring sites,<sup>34</sup> thus its high value for PIFPA can be taken as an indication of improved intermolecular coupling as compared to other conjugated polymers.

Charge transport in organic semiconductors is strongly dependent on the intermolecular charge transfer rates, which vary greatly with molecular packing parameters.<sup>35</sup> By utilizing  $\pi$ -stacking induced crystallization, a narrow distribution of packing parameters is achieved. However, the natural packing scheme of a molecular system does not necessarily match the packing scheme with maximum charge transfer rates. In Marcus-Hush theory based simulations for the intermolecular hole transfer rate, it has been reported that the lateral and torsional disorder in PFO can result in increased mobility as compared to highly ordered cases. The authors suggest that the disorder results in a larger distribution of intermolecular packing parameters and thus charge transfer rates, resulting in the formation of an efficient transport network based on interchain hops at locations with high transfer rates.<sup>36</sup> The portion of high transfer rate sites does not need to be high, as charge transport pathways in conjugated polymer thin films form through the sites with optimal transfer parameters, and the remainder of the thin film has little influence, as reported for P3HT-insulator blends that retain high mobility for up to 90 wt. % of insulating component.<sup>37</sup> In another example, dithienopyrrole-thiophene semicrystalline conjugated copolymers exhibit high mobilities of up to  $0.2$  cm<sup>2</sup>/Vs in as-cast low-order thin

films that drop by a factor of 2 to 20 upon annealing-induced crystallization.<sup>38</sup>

Given the lack of order in PIFPA, the above rationale can reasonably explain the strong intermolecular coupling indicated by the high prefactor mobility, and in combination with low energetic disorder, provides a basis for the high mobility of this amorphous conjugated copolymer and indicates that high mobilities (exceeding  $0.1$  cm<sup>2</sup>/Vs) are achievable without extensive  $\pi$ -stacking.

In summary, we have demonstrated FETs with a high mobility PIFPA amorphous copolymer, with an initial value of  $0.3$  cm<sup>2</sup>/Vs, stabilizing at  $0.25$  cm<sup>2</sup>/Vs after several weeks in air, and showing no detectable degradation for the next 5 weeks. AFM, DSC, and GIWAXS measurements revealed no detectable evidence of crystallinity in the copolymer thin films. High FET mobility is ascribed to low energetic disorder  $\sigma = 48$  meV along the semiconductor-insulator interface and strong intermolecular coupling indicated by high  $\mu_0 = 0.67$  cm<sup>2</sup>/Vs, explained by considering the presence of disorder-induced efficient intermolecular hole transfer sites that are probed during the measurements. Overall, PIFPA is a promising material for organic electronics applications since it rivals crystalline materials, including pentacene in terms of charge transport, but thin film formation is significantly simplified due to amorphous nature of this copolymer.

Funding for this work was provided by the Engineering and Physical Sciences Research Council UK and Merck Chemicals UK. We acknowledge G. Adamopoulos and W. P. Gillin (Queen Mary University of London) for their assistance in variable temperature measurements.

<sup>1</sup>S. K. Park, T. N. Jackson, J. E. Anthony, and D. A. Mourey, *Appl. Phys. Lett.* **91**, 063514 (2007).

<sup>2</sup>I. McCulloch, M. Heeney, C. Bailey, K. Genevicius, I. Macdonald, M. Shkunov, D. Sparrowe, S. Tierney, R. Wagner, W. Zhang, M. L. Chabinyc, M. D. McGehee, and M. F. Toney, *Nature Mater.* **5**, 328 (2006).

<sup>3</sup>H. Sirringhaus, *Proc. IEEE* **97**, 1570 (2009).

<sup>4</sup>H. Sirringhaus, *Adv. Mater.* **17**, 2411 (2005).

<sup>5</sup>H. Sirringhaus, M. Bird, T. Richards, and N. Zhao, *Adv. Mater.* **22**, 3893 (2010).

<sup>6</sup>Z. He, K. Xiao, W. Durant, D. K. Hensley, J. E. Anthony, K. Hong, S. M. Kilbey II, J. Chen, and D. Li, *Adv. Funct. Mater.* **21**, 3617 (2011).

<sup>7</sup>M. Mas-Torrent, P. Hadley, S. T. Bromley, X. Ribas, J. Tarres, M. Mas, E. Molins, J. Veciana, and C. Rovira, *J. Am. Chem. Soc.* **126**, 8546 (2004).

<sup>8</sup>J. M. Verilhac, M. Benwadih, A. L. Seiler, S. Jacob, C. Brory, J. Bablet, M. Heitzman, J. Tallal, L. Barbut, P. Frere, G. Sicard, R. Gwoziecki, I. Chartier, R. Coppard, and C. Serbutoviez, *Org. Electron.* **11**, 456 (2010).

<sup>9</sup>J. Veres, S. Ogier, and G. Lloyd, *Chem. Mater.* **16**, 4543 (2004).

<sup>10</sup>M. Hamsch, K. Reuter, M. Stanel, G. Schmidt, H. Kempa, U. Fugmann, U. Hahn, and A. C. Hubler, *Mater. Sci. Eng., B* **170**, 93 (2010).

<sup>11</sup>J. Lee, S. Cho, and C. Yang, *J. Mater. Chem.* **21**, 8528 (2011).

<sup>12</sup>O. D. Jurchescu, J. Baas, and T. T. M. Palstra, *Appl. Phys. Lett.* **84**, 3061 (2004).

<sup>13</sup>H. Sirringhaus, *Adv. Mater.* **21**, 3859 (2009).

<sup>14</sup>M. Uno, Y. Tominari, and J. Takeya, *Org. Electron.* **9**, 753 (2008).

<sup>15</sup>R. Hamilton, J. Smith, S. Ogier, M. Heeney, J. E. Anthony, I. McCulloch, J. Veres, D. D. C. Bradley, and T. D. Anthopoulos, *Adv. Mater.* **21**, 1166 (2009).

<sup>16</sup>D. M. De Leeuw, M. M. J. Simeon, A. R. Brown, and R. E. F. Einerhand, *Synth. Met.* **87**, 53 (1997).

<sup>17</sup>D. H. Kim, B. L. Lee, H. Moon, H. M. Kang, E. J. Jeong, J.-I. Park, K. M. Han, S. Lee, B. W. Yoo, B. W. Koo, J. Y. Kim, W. H. Lee, K. Cho, H. A. Becerril, and Z. Bao, *J. Am. Chem. Soc.* **131**, 6124 (2009).

<sup>18</sup>S. Georgakopoulos, D. Sparrowe, F. Meyer, and M. Shkunov, *Appl. Phys. Lett.* **97**, 243507 (2010).

- <sup>19</sup>H. Kempa, K. Reuter, M. Bartzsch, U. Hahn, A. C. Huebler, D. Zielke, M. Forster, and U. Scherf, in IEEE Polytronic Conference, Wroclaw, Poland (2005).
- <sup>20</sup>N. Schulte, R. Scheurich, and J. Pan, patent DE102006038683A1, Germany (2008).
- <sup>21</sup>D. E. Eastman, *Phys. Rev. B* **2**, 1 (1970).
- <sup>22</sup>T. J. Ha, D. Sparrowe, and A. Dodabalapur, *Org. Electron.* **12**, 1846 (2011).
- <sup>23</sup>H. Bassler, *Phys. Status Solidi B* **175**, 15 (1993).
- <sup>24</sup>H. Kim, N. Schulte, G. Zhou, K. Mullen, and F. Laquai, *Adv. Mater.* **23**, 894 (2011).
- <sup>25</sup>T. Kreouzis, D. Poplavskyy, S. M. Tuladhar, M. Campoy-Quiles, J. Nelson, A. J. Campbell, and D. D. C. Bradley, *Phys. Rev. B* **73**, 235201 (2006).
- <sup>26</sup>J. H. Worne, J. E. Anthony, and D. Natelson, *Appl. Phys. Lett.* **96**, 053308 (2010).
- <sup>27</sup>J. D. Yuen, R. Menon, N. E. Coates, E. B. Namdas, S. Cho, S. T. Hannahs, D. Moses, and A. J. Heeger, *Nature Mater.* **8**, 572 (2009).
- <sup>28</sup>S. F. Nelson, Y.-Y. Lin, D. J. Gundlach, and T. N. Jackson, *Appl. Phys. Lett.* **72**, 1854 (1998).
- <sup>29</sup>J. Veres, S. D. Ogier, S. W. Leeming, D. C. Cupertino, and S. Mohialdin Khaffaf, *Adv. Funct. Mater.* **13**, 199 (2003).
- <sup>30</sup>D. Hertel and H. Bassler, *ChemPhysChem.* **9**, 666 (2008).
- <sup>31</sup>R. U. A. Khan, D. Poplavskyy, T. Kreouzis, and D. D. C. Bradley, *Phys. Rev. B* **75**, 035215 (2007).
- <sup>32</sup>A. J. Mozer, N. S. Sariciftci, A. Pivrikas, R. Osterbacka, G. Juska, L. Brasat, and H. Bassler, *Phys. Rev. B* **71**, 035214 (2005).
- <sup>33</sup>A. R. Inigo, H. C. Chiu, W. Fann, Y. S. Huang, U. S. Jeng, T. L. Lin, C. H. Hsu, K. Y. Peng, and S. A. Chen, *Phys. Rev. B* **69**, 075201 (2004).
- <sup>34</sup>P. M. Borsenberger, *J. Appl. Phys.* **68**, 5188 (1990).
- <sup>35</sup>J. L. Bredas, J. P. Calbert, D. A. da Silva Filho, and J. Cornil, *Proc. Natl. Acad. Sci. U.S.A.* **99**, 5804 (2002).
- <sup>36</sup>S. Athanasopoulos, J. Kirkpatrick, D. Martinez, J. M. Frost, C. M. Foden, A. B. Walker, and J. Nelson, *Nano Lett.* **7**, 1785 (2007).
- <sup>37</sup>A. Kumar, M. A. Baklar, K. Scott, T. Kreouzis, and N. Stingelin-Stutzmann, *Adv. Mater.* **21**, 4447 (2009).
- <sup>38</sup>J. Liu, R. Zhang, G. Sauve, T. Kowalewski, and R. D. McCullough, *J. Am. Chem. Soc.* **130**, 13167 (2008).